

Band gap tuning in GaN through equibiaxial in-plane strains

L. Dong,¹ S. K. Yadav,² R. Ramprasad,^{1,2} and S. P. Alpay^{1,2,a)}

¹Department of Physics, University of Connecticut, Storrs, Connecticut 06269, USA

²Materials Science and Engineering Program and Institute of Materials Science, University of Connecticut, Storrs, Connecticut 06269, USA

(Received 19 March 2010; accepted 27 April 2010; published online 19 May 2010)

Structural transformations and the relative variation in the band gap energy (ΔE_g) of (0001) gallium nitride (GaN) films as a function of equibiaxial in-plane strains are studied by density functional theory. For relatively small compressive misfits (-6% – 0%), the band gap is estimated to be around its strain-free value, while for small tensile strains (0% – 6%), it decreases by approximately 45%. In addition, at large tensile strains ($>14.5\%$), our calculations indicate that GaN may undergo a structural phase transition from wurtzite to a graphitelike semimetallic phase. © 2010 American Institute of Physics. [doi:10.1063/1.3431290]

Gallium nitride (GaN) is a wide band gap ($E_g = 3.4$ eV) semiconductor that usually crystallizes in the wurtzite structure.¹ Its alloy with indium nitride (InN, $E_g = 0.7$ eV) has a band gap that is continuously tunable within the energy range of solar spectrum. Therefore, these materials may have promising applications in photovoltaics and light emission diodes (LEDs). The InGaN system has been intensively studied during the past decade.^{1,2} However, there still exist two fundamental problems. First, the external quantum efficiency of LEDs drops dramatically to an unacceptable level when the In molar fraction reaches 0.30, referred to as the “green valley of death.”² Second, a phase separation occurs at high In concentrations (0.32) due to the large atomic size mismatch between Ga and In.³ Thus, other methods to tune the band gap are needed for potential applications of GaN and related materials systems.

It is well-known that the structure and electronic properties of semiconductors can be altered by applying external stresses⁴ (such as hydrostatic pressure) or inducing internal strains⁵ (through lattice and/or thermal mismatch strains in thin films). In fact, “strain engineering” in semiconductors as well as functional materials has been widely employed to obtain desired physical and electrical properties.^{6–8} Interatomic distances and the relative positions of atoms have a strong bearing on the band structure and E_g in compound semiconductors. This makes it possible to control and tune E_g through in-plane misfit strains in epitaxial thin films. This concept is the main topic of this letter wherein we show using first principles calculations of appropriately strained GaN that its E_g can be adjusted by the lattice mismatch between an epitaxial GaN film and the underlying substrate. Furthermore, our results predict the formation of semimetallic phases for relatively large tensile or compressive in-plane strains.

Similar theoretical studies for InGaN nanowires show that there exists a strong relation between the dimensions of the nanowires, the strain energy, and the band gap.⁶ Very recently, Yadav *et al.*⁷ carried out a density functional theory (DFT) study of ZnX (X=O, S, Se, and Te) under uniaxial strain along the [0001] direction [or equivalently, equibiaxial

strains in the (0001) plane]. Their findings indicate that the band gap decreases for both compressive and tensile in-plane strains and that there exists a phase transition from wurtzite to a graphitelike phase at large compressive strains.

DFT simulations have been widely used in the past to predict properties of GaN under equilibrium conditions.^{9–12} The crystal structure, elastic constants, polarizations, and surface properties of GaN have been calculated by the local density approximation and generalized gradient approximation (GGA), in agreement with experimental data.^{9,10} However, E_g is typically underestimated to be around 1.7 eV (compared to the experimental value of 3.4 eV). While more recent time-intensive beyond DFT calculations^{11,12} involving exact-exchange functionals can reproduce the experimental value, the relatively simpler GGA is employed in our analysis because we focus mainly on the *relative variation* in E_g rather than its absolute value.

Here, we calculate the structural and electronic properties of GaN under equibiaxial in-plane strains in the (0001) plane to simulate GaN films with [0001] [*c*-axis, Fig. 1(a)] epitaxy. The simulations are performed using the VASP¹³ with the PW91 GGA,¹⁴ projector-augmented wave pseudopotentials,¹⁵ and a cutoff energy of 400 eV for the plane wave expansion of the wave functions. A Monkhorst-Pack *k*-point mesh of $9 \times 9 \times 9$ is used throughout the calculations to obtain well-converged results. The atom positions in the unit cell are relaxed until each component of the force is reduced below 0.02 eV/Å.

The wurtzite structure consists of alternating hexagonal closed-packed (0001) Ga and N layers [Fig. 1(a)]. Each Ga

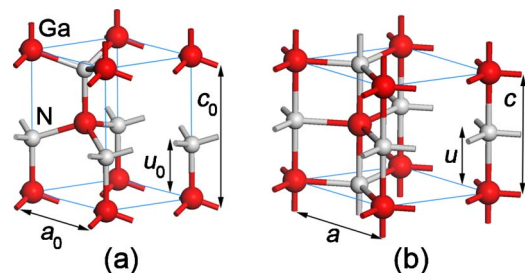


FIG. 1. (Color online) (a) Strain-free wurtzite unit cell and (b) graphitelike semimetallic phase unit cell under large compressive in-plane strains. The *c*-axis is along [0001] direction in each case.

^{a)}Author to whom correspondence should be addressed. Electronic mail: p.alpay@ims.uconn.edu.

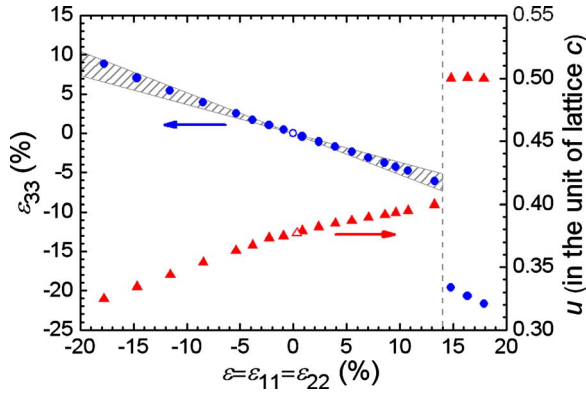


FIG. 2. (Color online) Out-of-plane strain ε_{33} and the internal lattice parameter u as a function of ε . The open circle and triangle represent the strain-free values. The wurtzite to graphitelike metallic phase occurs at $\varepsilon \equiv 14\%$ (dashed line).

(N) is nearly equidistant to its four nearest N (Ga) atoms which form a tetrahedron. The structure is characterized by an in-plane lattice parameter a , an out-of-plane lattice parameter c along the $[0001]$ direction, and an internal lattice parameter u , which is used to measure the interatomic distance along $[0001]$ axis (Fig. 1). The strain-free equilibrium lattice parameters a_0 , c_0 , and u_0 obtained from our calculations are 3.223 Å, 5.239 Å, and $0.377 \cdot c_0$, respectively, in excellent agreement with experimental findings (3.189 Å, 5.186 Å, and $0.377 \cdot c$) and previous calculations.⁹

In the presence of equibiaxial in-plane stresses, a certain value of the in-plane strain is specified which corresponds to a new lattice parameter a . This strain is given by $\varepsilon = \varepsilon_{11} = \varepsilon_{22} = (a - a_0)/a_0$ and the commensurate out-of-plane stress-free strain is $\varepsilon_{33} = (c - c_0)/c_0$. Therefore, the in-plane lattice parameter a (and as such ε) is taken as the parameter of the calculations and varied in our simulations from 2.65 to 3.80 Å, corresponding to $-17.8\% < \varepsilon < 17.9\%$. As shown in Fig. 2, for the wurtzite structures ($-17.8\% < \varepsilon < 14\%$), the calculated values of ε_{33} display approximately a linear response as a function of ε while u varies slightly nonlinearly from $0.325 \cdot c$ to $0.400 \cdot c$ in the same ε -range. The linear dependence of ε_{33} on ε can be easily understood through the Hooke's law as follows:

$$\sigma_{ij} = C_{ijkl} \cdot \varepsilon_{kl}, \quad (1)$$

which is reduced to the following:

$$\begin{pmatrix} \sigma_{11} & 0 & 0 \\ 0 & \sigma_{22} & 0 \\ 0 & 0 & 0 \end{pmatrix} = C_{ijkl} \cdot \begin{pmatrix} \varepsilon & 0 & 0 \\ 0 & \varepsilon & 0 \\ 0 & 0 & \varepsilon_{33} \end{pmatrix}. \quad (2)$$

In Eqs. (1) and (2), σ_{ij} , ε_{kl} , and C_{ijkl} are stress, strain, and elastic coefficients, respectively. We note that the mechanical boundary conditions require that all σ_{ij} except σ_{11} and σ_{22} are zero. Similarly, all ε_{kl} except ε_{kk} are zero and ε_{33} is a stress-free strain. Therefore, taking into account the anisotropy in the elastic coefficients, it can be easily shown that

$$\frac{\varepsilon_{33}}{\varepsilon} = -\frac{2C_{1133}}{C_{3333}}. \quad (3)$$

Previous experimental and theoretical results of the stiffness ratio of C_{1133}/C_{3333} fall into a range from 0.184 to 0.261, corresponding to $\varepsilon_{33}/\varepsilon$ from -0.364 to -0.522 .^{1,9,16} This range is shown as the shaded area in Fig. 2. Our calculations

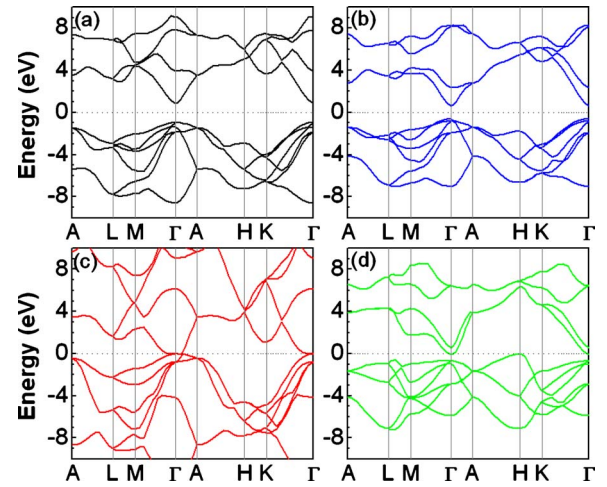


FIG. 3. (Color online) Band structure of GaN for (a) $\varepsilon = -3.8\%$; (b) $\varepsilon = 3.9\%$; (c) $\varepsilon = -17.8\%$; and (d) $\varepsilon = 14.8\%$. The crystal structures are wurtzite in [(a)–(c)], and the graphitelike phase in (d). Fermi level is set to be zero in each figure.

yield $\varepsilon_{33}/\varepsilon$ as -0.468 which is consistent with prior experimental findings.

More interestingly, there is a discontinuity in ε_{33} and u at $\varepsilon = 14.5\%$, corresponding to a phase transition from wurtzite [Fig. 1(a)] to a graphitelike phase [Fig. 1(b)]. The cation (anion) becomes coplanar with the three anions (cations) in the basal plane, thus resulting in $u = 0.5 \cdot c$. We note that this structure is slightly different from graphite because each cation (anion) has bonds with the two adjacent anions (cations) along the c -axis, in addition to bonds with three anions (cations) in the same plane. Our results indicate that when GaN is subjected to equibiaxial in-plane strains, the unit cell volume increases by 20% from $\varepsilon = 0\%$ to 14.5% followed by an abrupt 14% drop at the phase transition to the graphitelike phase (not shown).

The electronic properties of GaN are also modified by the misfit strains. Four band structures under different strains are plotted in Fig. 3. The band structures of (a)–(c) correspond to wurtzite structures which display direct band gaps, with both valence band minimum (VBM) and conduction band maximum (CBM) at Γ point. However, the graphitelike phase shows an “indirect” zero band gap semimetallic band structure [Fig. 3(d)]; the CBM is still at Γ point but the VBM now has shifted to H point.

At both large compressive and tensile in-planes strains [Figs. 3(c) and 3(d)], the Fermi level becomes equal to the CBM and VBM, introducing another important transition from semiconductor to semimetallic phases. The mechanism by which E_g becomes smaller is very similar to that of ZnX in Ref. 7. The VBM states of GaN are mainly occupied by the N p_x , p_y , and p_z orbitals, which overlap in a “degenerate” manner when GaN is strain-free. But under strain, the p_z orbital would split away from the p_x and p_y orbitals. However, we note that these are purely bulk calculation results. For ultrathin films with a thickness of 10–100 Å, the surface electron accumulation by defect states would raise the Fermi level to the upper part of the band gap¹⁷ and the CBM would reach the Fermi level at a smaller in-plane strain. Hence, it should be easier to obtain the metallic phase in thin film GaN.

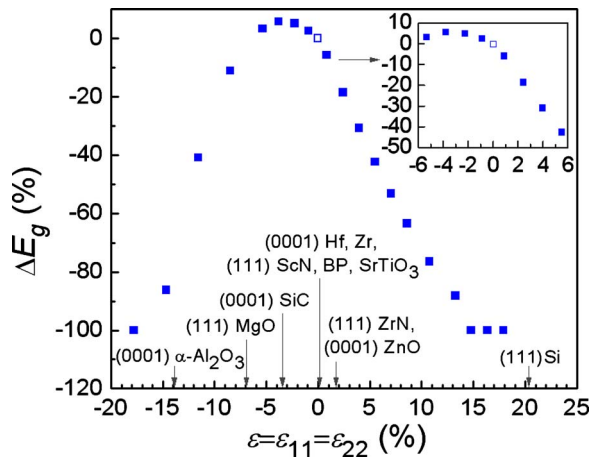


FIG. 4. (Color online) Relative variation in band gap ΔE_g with ε . The in-plane strain between some commercially available substrate materials and GaN are marked on the figure. The inset shows ΔE_g as a function of ε for $-6\% < \varepsilon < 6\%$.

Our results show that E_g of strain-free GaN is 1.709 eV. The relative variation in the band gap ΔE_g with respect to the $E_g(\varepsilon=0)$ as a function of ε is shown in Fig. 4. The band gap tuning is asymmetric with respect to the sign of the in-plane strain. For $-6\% < \varepsilon < 0$, E_g increases only by 6%. Beyond this range, E_g drops dramatically to 0 eV ($\Delta E_g = -100\%$) at $\varepsilon = -17\%$. On the other hand, for tensile in-plane strains, ΔE_g is negative, and varies linearly with strain. Relatively small tensile strains result in a significant narrowing of the gap such that $\Delta E_g = -42.4\%$ for $\varepsilon = 5.5\%$. E_g (under tensile strains) reaches a zero value when the transformation to the graphitelike phase is complete. We note that although DFT underestimates the absolute value of the band gap, trends in band gap value changes are well predicted by DFT. For instance, pressure coefficients of the band gap computed using DFT are in excellent agreement with experiments, and trends in relative variations in band gaps computed using different levels of theory are in mutual agreement with each other.⁷

We thus expect that appropriate equibiaxial strains in ultrathin pseudomorphic GaN films on suitable substrates may be used to “tune” the GaN band gap to span the solar spectrum, thereby enabling a number of important technological applications. For instance, to result in a band gap value in the blue to green light region ($-42.5\% < \Delta E_g < -19.0\%$), substrates with 2.5%–5.5% lattice mismatch would be needed. This would require substrate materials with lattice parameters in the range of 3.273–3.369 Å and with similar thermal expansion parameters as GaN. A number of materials were investigated as potential substrates for epitaxial GaN such that appropriate levels of in-plane stresses may be imposed. The lattice mismatch between commercially avail-

able substrates and epitaxial pseudomorphic GaN films are marked on Fig. 4, and more are listed in Ref. 18. We note that epitaxial stresses may be relaxed by the formation of misfit dislocations at the film substrate interface. The equilibrium critical thickness for the formation of misfit dislocations (h_p) in epitaxial GaN films can be determined using the Matthews–Blakeslee (MB) criteria.¹⁹ For wurtzite films, taking the Burgers vector and the dislocation line as $1/3[\bar{1}2\bar{1}0]$ and $[2\bar{1}\bar{1}0]$, respectively,²⁰ and a deposition temperature of $T_G = 650$ °C, we can determine the critical thickness h_p as a function of the pseudomorphic misfit at T_G . The results show that as the magnitude of the strain increases from 2% to 6%, h_p decreases from 30 to 5 Å. For larger strains, h_p from MB criteria should be expected to be less than one unit cell although the film may grow via island coalescence rather than the MB assumption of layer-by-layer growth. Although the range of strains considered here is enormous, appreciable changes (i.e., reductions) in the band gap may be accomplished for modest and realistic strains. Finally, we note that the theory developed in this letter can be validated through deposition of epitaxial (0001) GaN on (0001) ZnO or (111) ZrN which would generate in-plane strains of about 1.8% in pseudomorphic films of GaN, resulting in a band gap reduction of about 15%.

¹I. Vurgaftman and J. R. Meyer, *J. Appl. Phys.* **94**, 3675 (2003).

²J. Wu, *J. Appl. Phys.* **106**, 011101 (2009).

³N. Li, S. Wang, E. Park, Z. Feng, H. Tsai, J. Yang, and I. Ferguson, *J. Cryst. Growth* **311**, 4628 (2009).

⁴W. B. Holzapfel, *Rep. Prog. Phys.* **59**, 29 (1996).

⁵G. C. Osbourn, *J. Appl. Phys.* **53**, 1586 (1982).

⁶H. J. Xiang, S. Wei, J. F. Da Silva, and J. Li, *Phys. Rev. B* **78**, 193301 (2008).

⁷S. K. Yadav, T. Sadowski, and R. Ramprasad, *Phys. Rev. B* **81**, 144120 (2010).

⁸D. Schlom, L. Chen, C. Eom, K. Rabe, S. Streiffer, and J. Triscone, *Annu. Rev. Mater. Sci.* **37**, 589 (2007).

⁹A. Zoroddu, F. Bernardini, P. Ruggerone, and V. Fiorentini, *Phys. Rev. B* **64**, 045208 (2001).

¹⁰A. L. Rosa and J. Neugebauer, *Phys. Rev. B* **73**, 205346 (2006).

¹¹P. Rinke, M. Scheffler, A. Qteish, M. Winkelkemper, D. Bimberg, and J. Neugebauer, *Appl. Phys. Lett.* **89**, 161919 (2006).

¹²X. Wu, E. Walter, A. Rappe, R. Car, and A. Selloni, *Phys. Rev. B* **80**, 115201 (2009).

¹³G. Kresse and J. Furthmüller, *Phys. Rev. B* **54**, 11169 (1996).

¹⁴J. P. Perdew, J. A. Chevary, S. H. Vosko, K. A. Jackson, M. R. Pederson, D. J. Singh, and C. Fiolhais, *Phys. Rev. B* **46**, 6671 (1992).

¹⁵P. E. Blöchl, *Phys. Rev. B* **50**, 17953 (1994).

¹⁶A. F. Wright, *J. Appl. Phys.* **82**, 2833 (1997).

¹⁷W. Walukiewicz, *Physica B* **302–303**, 123 (2001).

¹⁸S. Kukushkin, A. Osipov, V. Bessolov, B. Medvedev, V. Nevolin, and K. Tcarik, *Rev. Adv. Mater. Sci.* **17**, 1 (2008).

¹⁹J. W. Matthews and A. E. Blakeslee, *J. Cryst. Growth* **27**, 118 (1974).

²⁰A. M. Sánchez, J. G. Lozano, R. García, M. Herrear, S. Ruffenach, O. Briot, and D. González, *Adv. Funct. Mater.* **17**, 2588 (2007).